ORIGINAL RESEARCH

Sella Turcica Area and Location of Point Sella in Cephalograms Acquired with Simulated Patient Head Movements

Olesya Svystun[1], Lars Schropp[2], Ann Wenzel[3], Rubens Spin-Neto[4]

Abstract

Aim and objective: This study assesses changes in the sella turcica area (STA) and location of the cephalometric point sella (S) on lateral cephalograms acquired by charge-coupled device (CCD)-based cephalostats with and without simulated patient head movements.

Materials and methods: A real skull was placed on a robot, able to simulate four head movements (anteroposterior translation/lifting/nodding/lateral rotation) at three distances (0.75/1.5/3 mm) and two patterns (returning to 0.5 mm away from the start position/staying at maximum movement excursion). Two ProMax-2D cephalostats (Dimax-3, D-3 or Dimax-4, D-4), and an Orthophos-SL cephalostat (ORT) acquired cephalograms during the predetermined movements ("cases," 48 images/unit) and without movement ("controls," 24 images/unit). Three observers manually traced the contour of sella turcica and marked point sella using a computer mouse. STA was calculated in pixels^2 by dedicated software based on the tracing. S was defined by its *x* and *y* coordinates recorded by the same software in pixels. Ten percent of the images were assessed twice. The difference between cases and controls (case *minus* control) for the STA and S (namely Diff-STA and Diff-S) was calculated and assessed through descriptive statistics.

Results: Inter- and intraobserver agreement ranged from moderate to good for STA and S. Diff-STA ranged from −42.5 to 12.9% (D-3), −15.3 to 9.6% (D-4), and −25.3 to 39.9% (ORT). Diff-S was represented up to 50% (D-3), 134% (D-4), and 103% (ORT) of the mean sella turcica diameter in control images.

Conclusion: Simulated head movements caused significant distortion in lateral cephalograms acquired by CCD-based cephalostats, as seen from STA and S alterations, depending on the cephalostat.

Clinical significance: Patient-related errors, including patient motion artifacts, are influential factors for the reliability of cephalometric tracing.

Keywords: Cephalogram, Digital image, Distortion, Sella turcica.

The Journal of Contemporary Dental Practice (2021): 10.5005/jp-journals-10024-3056

Introduction

Sella turcica is a saddle-shaped depression in the body of the sphenoid bone of the skull, which serves as a critical cephalometric landmark for dentofacial and neurocranial morphological measurements.[1] The shape of sella turcica can be circular, oval, or flat. The most common types, however, are circular and oval.[2,3] Studies have focused on the location, morphology, and size of the sella turcica for routine cephalometric analysis.[3,5] When considered in cephalometric analyses, sella turcica is referred to as point sella (S), and is defined manually (and subjectively).[6] Point sella is defined as the midpoint of sella turcica, as located on a cephalogram,[6] and is relevant for defining sagittal jaw relations for cephalometric measurements.[4] The morphology of sella turcica impacts the definition of S during the evaluation of cranial morphology, estimation of growth changes, and evaluation of orthodontic treatment results. There is a significant correlation between linear/area measurements and the age of the patient.[2] During skeletal growth, changes occur in the shape and size of sella turcica, and S is being displaced backward and downward during growth and development.[4,7] Abnormalities in sella turcica can be associated with several developmental abnormalities within the craniofacial region.[1]

A traditional cephalogram is a two-dimensional (2D) summation image of the skull and facial structures, obtained in a cephalostat. The image makes it possible to locate anatomical structures, which are used to analyze morphologic relations, establish a treatment plan, follow up during treatment, and for the eventual control of treatment.[8] Digital cephalostats may vary in the techniques for image capture and provide different spatial resolutions in the image.[9] Most digital cephalostats imply that a collimator with a thin slit opening exposes the patient during a continuous examination, lasting approximately 12 seconds, working either horizontally (covering the nose–neck direction) or vertically (top of the head to the chin direction).[10,11]

In digital cephalostats, the sensors are often smaller than the expected field of view of the final cephalogram, and therefore the final image is constructed of data captured by a sensor that is

[1-4]Department of Dentistry and Oral Health, Aarhus University, Aarhus, Denmark

Corresponding Author: Rubens Spin-Neto, Department of Dentistry and Oral Health, Aarhus University, Aarhus, Denmark, e-mail: rsn@dent.au.dk

How to cite this article: Svystun O, Schropp L, Wenzel *A, et al*. Sella Turcica Area and Location of Point Sella in Cephalograms Acquired with Simulated Patient Head Movements. J Contemp Dent Pract 2021; 22(3):207–214.

Source of support: Nil

Conflict of interest: None

composed of two or more parts. When the image segments from these separate sensor parts are stitched to compose a single image, image-stitching artifacts may occur.[10,11] Young patients have a tendency to move during long-lasting radiographic examinations,[12] which might affect the images from two (or more) sensors and lead to stitching line artifacts and distortion.[11] A recent study found these artifacts to be more prevalent in children, speculating that patient movement could be related to the presence of these artifacts.[10] These artifacts may affect the clinical use of cephalograms because their presence could influence image interpretability and cephalometric analysis.[10]

The aim of the present study is to assess changes in the sella turcica area (STA) and location of the cephalometric point sella (S) in lateral cephalograms acquired by charge-coupled device (CCD)-based cephalostats of two types, single and dual sensor, and the relation between these parameters and simulated head movements.

Materials and Methods

The study was performed at the Department of Dentistry and Oral Health, Aarhus University, Denmark. The used skull belongs to the department acervus.

Robot Movements

A dentate human skull embedded in wax to simulate soft tissues[13] was mounted on a robot (UR10, Universal Robots, Odense, Denmark). The robot was programmed to reproduce four head movement types (anteroposterior translation, head lifting, nodding, and lateral rotation), which were selected based on the clinical evidence, i.e., movements previously observed to be performed by patients during extraoral radiographic examinations.[12]

The performance was dependent on the rotation of joints of the robot. The angles were adjusted to provide movement distances of 0.75, 1.5, and 3 mm, when measured at the skull's anterior nasal spine. Movements were occurred at a speed of 5 mm/second (e.g., fast head movements) and lasted a maximum of 0.6 seconds. The movements started at the midpoint of the exposure trajectory, besides the skull. Two movement patterns were performed: (1) the skull returned to a position located 0.5 mm away from the start position after reaching the maximum excursion for the movement ("returning"), and (2) the maximum excursion of the movement defined its end ("not returning"). No-motion control images were acquired, with the robot set to the start position and inactive.

Image Acquisition

Three digital cephalostats—two ProMax-2D (Planmeca Oy, Finland), one with a Dimax-3 (D-3) and one with a Dimax-4 (D-4) CCD sensor, and one Orthophos-SL unit (ORT, Dentsply Sirona, Germany)—were used to acquire lateral cephalograms of the skull. In D-3 and D-4, image segments (an upper and a lower) from two separate CCD sensors were blended (i.e., stitched) to compose the final full image. In ORT, the images originate from a single CCD sensor. Images were acquired during the predetermined movements (in duplicate, totaling 48 images/unit, the "cases") and without movement (one image after each pair of equal images acquired with movement, totaling 24 images/unit, the "controls").

The cephalostats were set to operate at 62 kV and 4 mA, and the cephalograms were acquired in the maximum available field of view, 28 x 26 cm (D-3), 26 x 24 cm (D-4), and 29 x 22 cm (ORT), in a resolution of 200 dpi (D-3 and D-4) and 244 dpi (ORT). Exposure time was 12 seconds for D-3, 10.5 seconds for D-4, and 14.9 seconds for ORT. The sensor position when starting the examination was at the nose end of the skull, and the sensor and X-ray tube moved backward horizontally during image acquisition. This acquisition pattern was the same for all three units. The robot program was personalized for each unit to perform the selected movement precisely when the sensor reached the center of the skull. The exported images and their relation with the performed movement were saved. Images were exported as BMP (bitmap) files.

The images were pseudonymized using a random, software-generated numerical sequence. Observers were blinded to the presence/absence and type of movement in the images. However, the observers were aware of the different cephalometric units based on the image resolution and the characteristics of the images.

Image Tracing

Three observers (two dental students and a Ph.D. student in oral radiology, trained and calibrated to perform requested tasks) viewed the images on a 24-inch monitor (Dell P2412H, Dell Inc., Round Rock, Texas, USA) in a room with dimmed light. Using dedicated image processing software (ImageJ, NIH, Bethesda, Maryland, USA), the observers manually traced the contours of the sella turcica with the computer mouse from the medial to the lateral border, after which the program connected the borders with a line (Fig. 1). Based on the tracing, the STA was automatically calculated by the software in pixels^2. Immediately after the area was calculated, the traced contours disappeared from the image. In the sequence, point sella was marked manually, also with the computer mouse. The software provided *x* and *y* coordinates of the marked point S in pixels. STA and S were saved in a separate spreadsheet, according to the image number. To evaluate intraobserver reproducibility, 10% of the sample was traced/marked twice (2 weeks between the first and second tracing/marking round). Working sessions were limited to approximately 2 hours per day to avoid observer fatigue.

Data Treatment

Statistical software (SPSS 24, IBM Corp., New York, New York) was used for data evaluation. Intra- and interobserver agreements were assessed by means of intraclass correlation coefficient (ICC) statistics.

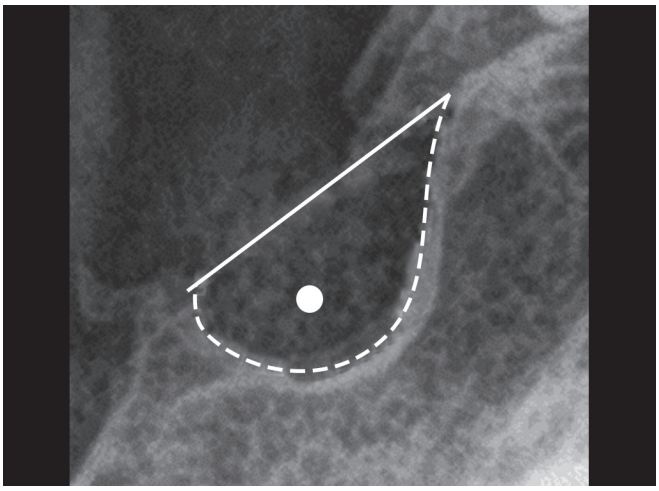

Fig. 1: Sella turcica area (STA, dashed line made by tracing with the computer mouse and solid line automatically drawn by the software) and the cephalometric point sella (S, white dot), as traced/marked by the observer in a control cephalogram (ORT)

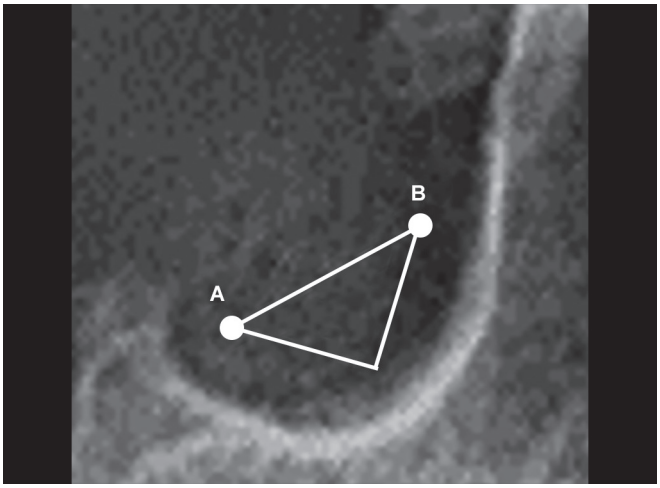

Fig. 2: Diff-S was calculated as a triangle's hypotenuse. *A* and *B* represent *S* on a case and a control image

The numerical difference between STA in the case image and STA in the corresponding control image (i.e., STA for the case *minus* STA for the control) was calculated (Diff-STA) in pixels^2. Considering point S in the case image ("point A," $x_a y_a$) and in the control image ("point B," $x_b y_b$), the coordinate difference AB (Diff-S, the distance between *S* marked in the case and in the control image, Fig. 2), was calculated with the formula: $AB = \sqrt{(x_a - x_b)\times(x_a - x_b)+(y_a - y_b)\times(y_a - y_b)}$, in pixels. As there were two cases for each control, the average of the two Diff-STA and the two Diff-S values represented each case (according to movement type, distance, and pattern per unit).

Diff-STA values were presented in a native-measuring unit (pixels^2), and the extreme values (i.e., largest decreases and increases in STA) were also presented as percentage of average STA in control images (Diff-STA/average $STA_{control} \times 100$). Diff-S values were presented in the native-measuring unit (pixels), and the extreme values were also presented as percentage of the average sella turcica diameter in control images ($Diameter = 2 \times \sqrt{STA \div \pi}$, in pixels). Diff-S values larger than 10% were defined as threshold for relevant variations in the sella location.[14]

Results

Inter- and intraobserver agreements (ICC values) ranged from moderate to good for STA (mean 0.817, range 0.767–0.871, and mean 0.868, range 0.832–0.901, respectively) and S (mean 0.756, range 0.623–0.815, and mean 0.741, range 0.698–0.831).

For D-3, the mean STA among observers was 3623 (range 3144–4927) pixels^2 in control images, and 3580 (range 1404–5108) pixels^2 in case images. Diff-STA ranged from −1539 to 466.50 pixels^2. Diff-STA value was positive for approximately half of the cases. The smallest Diff-STA represented a decrease (i.e., STA was smaller than the average of control STA) equal to 42.5% of average STA for the control images, while the largest Diff-STA represented an STA increase (i.e., STA was larger than the average of control STA) of 12.9%. Diff-S ranged from 0.47 to 34.31 pixels, which corresponds to a range of 0.32 to 50% of the average sella turcica diameter in control images, which was 68 pixels. In 42% of the cases, Diff-S was larger than 10% of the sella turcica diameter in control images. Diff-S was more often increased for the anteroposterior translation and head lifting movement types. Further, the returning movement pattern was more often associated with cases of Diff-S larger than 10% of the average sella turcica diameter. However, no trends were seen for movement distance. Diff-STA and Diff-S values for D-3 are presented in Table 1. Figure 3 presents visible changes in sella turcica shape in case and control images acquired with D-3.

For D-4, the mean STA among observers was 3089 (range 2801–3560) pixels^2 in control images, and 3069 (range 2697–3457) pixels^2 in case images. Diff-STA presented a range from −474 to 296.50 pixels^2. The smallest Diff-STA represented a decrease equal to 15.3% of the average STA for the control images, while the largest Diff-STA represented an increase of 9.6%. Diff-STA indicated that STA was smaller than the average of control images in approximately 60% of the cases. The largest Diff-S was 84.39 pixels, which corresponds to 134% of average sella turcica diameter in control images (62.73 pixels). In 25% of the cases, Diff-S values were larger than 10% of average sella turcica diameter in control images. Larger Diff-S values were more often associated with head lifting movement and the longest distance (3 mm) of the lateral rotation movement in the not-returning pattern. Diff-STA and Diff-S values for D-4 are presented in Table 2. Figure 4 presents changes in sella turcica shape in case and control images acquired with D-4.

For ORT, the mean STA among observers was 5649 (range 4676–6557) pixels^2 in control images and 5737 (range 3925–7959) pixels^2 in case images. Diff-STA ranged from −781 to 1231 pixels^2. The smallest Diff-STA represented a decrease equal to 25% of the average STA for the control images, while the largest diff-STA represented an increase of 40%. Diff-STA value was negative for approximately half of the cases. Diff-S ranged from 0 to 70.65 pixels, which corresponds to 103% of the average sella turcica diameter in control images (69 pixels). Diff-S values of more than 10% of the average sella turcica diameter in control images represented 92% of the cases. There were no definite trends as to which movement types, distances, or patterns were associated with larger Diff-STA and Diff-S. Diff-STA and Diff-S values for ORT are presented in Table 3. Figure 5 presents changes in sella turcica shape in case and control images acquired with ORT.

Discussion

The anatomical structures of the skull must be correctly reproduced in lateral cephalograms. This assures a true representation of the patient's anatomy, allowing a more precise cephalometric analysis, assisting with the orthodontic treatment planning.[14] Despite the fast development of artificial intelligence solutions for cephalometric analysis, anatomic landmarks in digital images are still mostly marked manually with the aid of a computer mouse.[15] This adds certain subjectivity to the procedure.[16] As suggested by Riedel, the subjectivity in the identification of orthodontic landmarks is the major cause of error in cephalometric analysis.[17] Also, even minor changes in the cephalometric angles [e.g., angle between sella, nasion, and subspinale point A and angle between sella, nasion, and supramentale point B] might lead to changes in patients' diagnosis and treatment.[18,19] Therefore, defining the possible causes of error when performing a cephalometric analysis is extremely relevant in the clinic. As reported by Schulze et al., when discussing cone-beam computed tomography (CBCT), patient-/object-, observer-, and equipment-related errors (pre- and post-process)[20] might be the main causes for image artifacts. The same applies to cephalograms. As Durão et al. concluded, these factors can also lead to the lack of precision in marking orthodontic landmarks.[21] To the present, patient movement has not been considered an influential factor for the reliability of cephalometric tracing.

Table 1: Diff-STA and Diff-S for D-3

			Observer 1		*Observer 2*		*Observer 3*	
			Pattern		*Pattern*		*Pattern*	
D-3	*Type*	*Distance (mm)*	*Not-returning*	*Returning*	*Not-returning*	*Returning*	*Not-returning*	*Returning*
Diff-STA (pixels^2)	APT	0.75	−3.50	−494.50	−55.46	104.00	3.00	−58.50
		1.50	−476.50	−314.00	−58.50	7.50	−135.50	65.00
		3.00	−543.50	−109.50	96.50	140.50	26.00	96.00
	HL	0.75	−57.00	108.00	76.13	−0.50	78.50	385.00
		1.50	254.50	466.50	−113.50	−109.50	−4.00	95.50
		3.00	6.50	34.00	−88.00	−150.50	310.50	−173.00
	NOD	0.75	−245.00	162.50	−20.26	−108.00	−198.50	176.00
		1.50	−422.00	190.50	−30.00	132.50	42.00	113.50
		3.00	−83.00	82.00	−51.00	58.50	152.50	−114.00
	LR	0.75	−54.50	−689.50	−83.88	−128.50	96.00	110.50
		1.50	−1366.00	−848.50	−283.50	−158.00	−6.50	259.50
		3.00	−398.50	−1539.00	−115.50	−740.00	−195.00	−302.50
Diff-S (pixels)	APT	0.75	4.95	11.77	2.90	11.95	2.82	13.26
		1.50	3.16	9.95	4.14	7.07	4.60	6.86
		3.00	5.29	8.15	5.06	5.91	5.32	6.09
	HL	0.75	10.37	34.31	7.86	10.56	7.70	11.40
		1.50	12.86	5.99	10.66	8.99	11.94	8.18
		3.00	1.58	7.88	5.29	11.96	5.34	13.27
	NOD	0.75	3.96	12.12	5.22	10.95	5.79	11.93
		1.50	3.16	2.29	5.48	2.19	6.08	2.13
		3.00	12.71	33.19	0.47	4.91	0.49	5.06
	LR	0.75	3.12	1.73	2.98	15.18	2.92	16.39
		1.50	8.09	3.73	5.36	2.20	6.00	2.00
		3.00	1.22	7.34	1.39	9.20	1.54	10.21

Diff-S values, which represent more than 10% of the average sella turcica diameter in the control images, are highlighted in gray. APT; anteroposterior translation, HL; head lifting, NOD; nodding, LR; lateral rotation

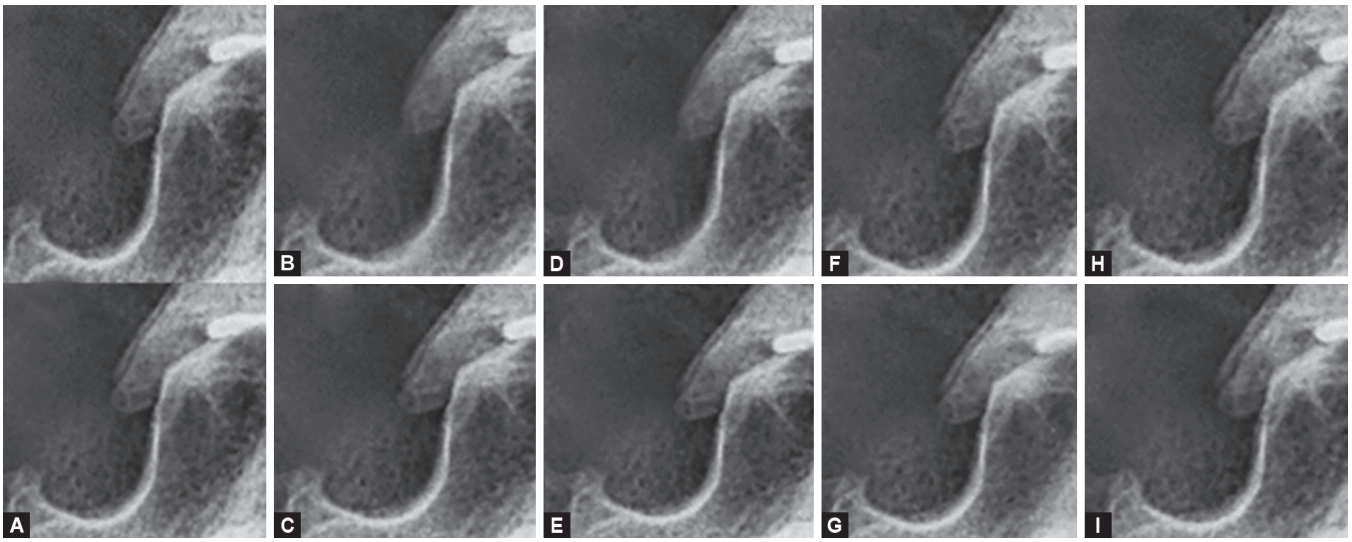

Fig. 3: Sella turcica acquired by D-3. A—control; B and C—1.5 mm anteroposterior translation (B: returning, C: not-returning); D and E—1.5 mm head lifting (D: returning, E: not-returning); F and G—1.5 mm nodding (F: returning, G: not-returning); H and I—1.5 mm lateral rotation (H: returning, I: not-returning)

Table 2: Diff-STA and Diff-S for D-4

			Observer 1		*Observer 2*		*Observer 3*	
			Pattern		*Pattern*		*Pattern*	
D-4	*Type*	*Distance (mm)*	*Not returning*	*Returning*	*Not returning*	*Returning*	*Not returning*	*Returning*
Diff-STA (pixels^2)	APT	0.75	−89.50	−474.00	−46.50	60.00	−100.00	78.00
		1.50	−435.50	−48.50	−27.00	−103.50	−5.00	−93.00
		3.00	−10.00	−262.00	−114.00	−195.00	−46.00	−72.50
	HL	0.75	75.50	−169.50	69.00	22.50	68.50	303.50
		1.50	107.50	238.50	−379.00	−103.00	−20.00	25.50
		3.00	296.50	124.00	24.00	27.00	−36.00	9.00
	NOD	0.75	315.50	−45.00	−1.78	−83.50	52.00	−175.50
		1.50	−260.50	−232.00	−112.50	−196.50	−39.50	41.50
		3.00	104.50	−168.00	35.50	−24.50	−54.00	77.50
	LR	0.75	258.00	281.00	−63.00	−107.00	47.50	−44.50
		1.50	−53.00	141.00	−16.00	0.00	−165.00	−183.50
		3.00	203.50	36.00	2.50	−186.00	44.50	−1.50
Diff-S (pixels)	APT	0.75	1.00	1.00	2.69	2.5	2.82	2.57
		1.50	26.89	3.25	2.05	4.5	2.01	4.86
		3.00	1.41	1.00	1.48	3.27	2.06	2.97
	HL	0.75	0	1.00	5.31	2.81	5.36	3.12
		1.50	43.19	45.40	17.92	77.42	38.20	84.39
		3.00	42.79	0	20.52	2.31	35.46	2.56
	NOD	0.75	1.22	0	1.44	1.67	1.57	1.68
		1.50	4.90	3.15	1.2	1.84	1.23	2.04
		3.00	7.48	2.58	6.29	1.00	6.76	1.05
	LR	0.75	4.54	1.41	1.91	6.91	1.74	6.78
		1.50	1.58	2.22	1.89	4.31	2.10	4.83
		3.00	47.53	0	44.36	1.94	48.35	1.95

Diff-S values, which represent more than 10% of the average sella turcica diameter in the control images, are highlighted in gray. APT; anteroposterior translation, HL; head lifting, NOD; nodding, LR; lateral rotation

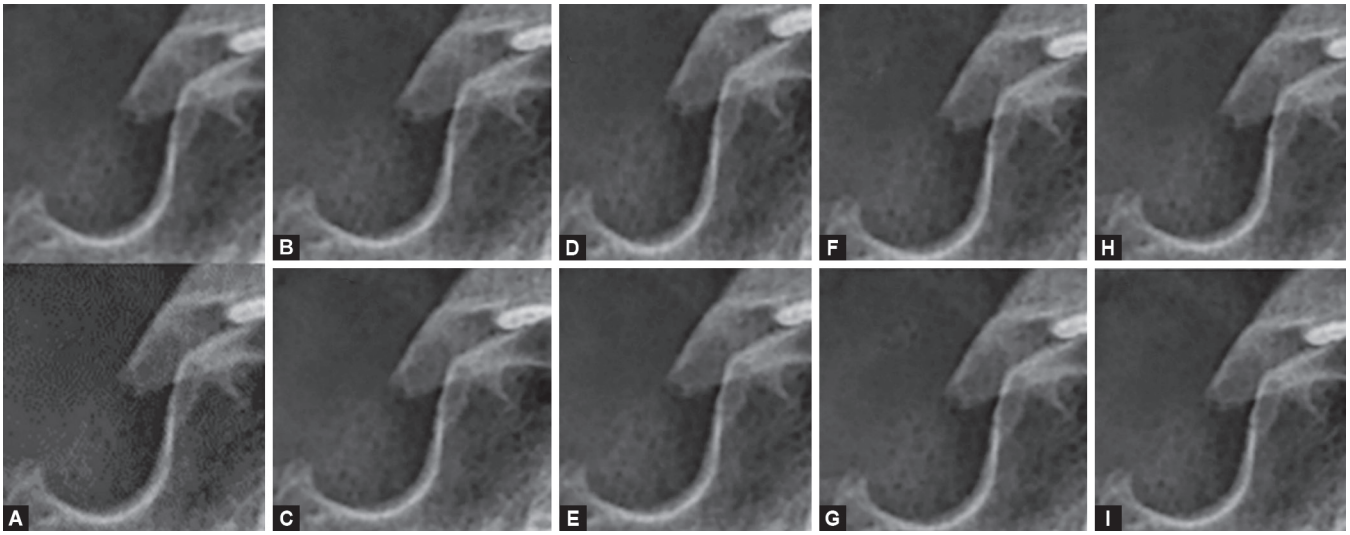

Fig. 4: Sella turcica acquired by D-4. A—control; B and C—1.5 mm anteroposterior translation (B: returning, C: not-returning); D and E—1.5 mm head lifting (D: returning, E: not-returning); F and G—1.5 mm nodding (F: returning, G: not-returning); H and I—1.5 mm lateral rotation (H: returning, I: not-returning)

Table 3: Diff-STA and Diff-S for ORT

ORT	*Type*	*Distance (mm)*	*Observer 1*		*Observer 2*		*Observer 3*	
			Pattern		*Pattern*		*Pattern*	
			Not returning	*Returning*	*Not returning*	*Returning*	*Not returning*	*Returning*
Diff-STA (pixels^2)	APT	0.75	89.50	−5.00	73.55	622.50	−65.50	96.00
		1.50	35.50	1231.00	−385.50	842.50	−686.00	661.50
		3.00	−363.50	943.00	−108.50	1169.50	−361.50	572.50
	HL	0.75	293.50	482.00	−23.28	−355.00	−108.00	−308.00
		1.50	−139.00	−349.50	278.50	−467.00	83.50	187.50
		3.00	302.50	−94.00	719.00	444.00	581.50	50.00
	NOD	0.75	426.00	−265.00	−139.93	−601.00	−69.50	−495.00
		1.50	−579.50	−256.00	−1170.00	−120.00	−781.00	186.00
		3.00	−583.50	1222.50	856.05	607.00	1059.5	566.5
	LR	0.75	99.00	−114.00	−21.35	−299.50	−207	−418.5
		1.50	105.50	530.50	−32.00	384.50	14.5	−103.5
		3.00	388.50	−140.50	613.50	−255.50	226.0	−295.5
Diff-S (pixels)	APT	0.75	70.65	28.57	69.04	63.91	69.73	67.57
		1.50	16.64	6.98	12.93	7.19	12.55	7.84
		3.00	0	11.38	7.61	6.31	7.69	7.01
	HL	0.75	8.72	22.79	41.31	44.88	42.55	48.92
		1.50	11.96	13.55	25.10	7.78	27.10	8.16
		3.00	41.33	60.21	31.00	48.80	40.73	64.66
	NOD	0.75	54.37	20.49	53.50	18.35	60.48	20.55
		1.50	8.93	34.48	15.98	20.18	17.42	20.39
		3.00	32.88	30.95	45.51	36.56	47.78	35.47
	LR	0.75	46.83	63.57	16.56	49.98	17.39	51.48
		1.50	46.42	29.49	44.19	8.56	43.31	9.24
		3.00	2.74	3.87	8.78	3.42	9.83	3.11

Diff-S values, which represent more than 10% of the average sella turcica diameter in the control images, are highlighted in gray. APT; anteroposterior translation, HL; head lifting, NOD; nodding, LR; lateral rotation

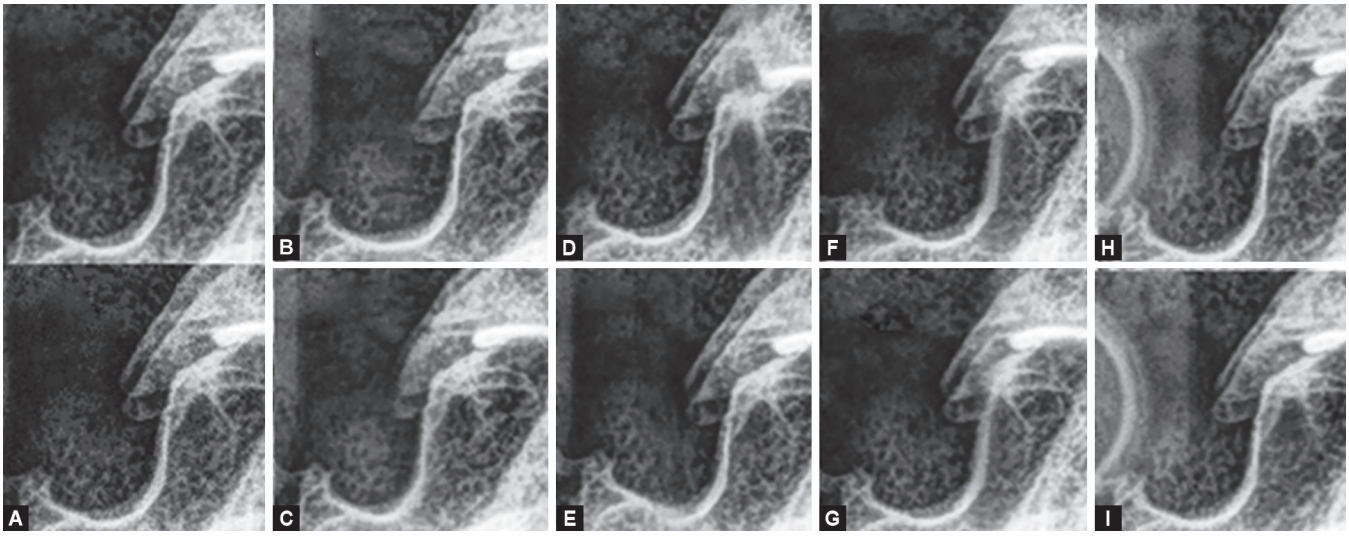

Fig. 5: Sella turcica acquired by ORT. A—control; B and C—1.5 mm anteroposterior translation (B: returning, C: not-returning); D and E—1.5 mm head lifting (D: returning, E: not-returning); F and G—1.5 mm nodding (F: returning, G: not-returning); H and I—1.5 mm lateral rotation (H: returning, I: not-returning)

In a recent study, Svystun et al. showed that up to 20% of images from cephalostats with dual CCD sensors have artifacts that might be caused by movements.[10] It has been shown that image-stitching artifacts, visualized as stitching lines, might lead to misalignment of the anatomical structures in the image in up to 75% of the cases.[10] The same study showed that these artifacts were more prevalent in children, and a relationship was suggested between patient movement during the examination and the presence and severity of artifacts.[10] Another study by the same group of researchers explored the presence and severity of image-stitching artifacts and distortion in lateral cephalograms acquired by CCD-based cephalostats of two types, single and dual.[11] The relation between image distortion and simulated head movement was also assessed.[11] The authors found that 3-mm movements, based on a returning pattern, led to a considerable number of severe artifacts in the images.[11] Therefore, it is reasonable to speculate that structures like sella turcica could suffer from major distortion in the presence of patient movements. As described by Oktay, universally, sella turcica–related characteristics and landmarks are considered difficult to identify.[22]

In the present study, movements in all planes (i.e., axial, coronal, and sagittal) were tested to uncover the influence of movements in combination with the three cephalostats. The selected movement distances reflect patient breathing movements (0.75 mm) and larger unintentional movements (1.5–3 mm).[12,23] The study design also takes into consideration other studies that have tracked patient movement during the acquisition of extraoral images (i.e., CBCT). These studies, performed by Spin-Neto and collaborators, suggested that a high percentage of patients younger than 15 years move to the largest distance (3 mm) selected in this study during long-lasting examinations.[12,24]

Even though the agreement among the observers ranged from moderate to good, the range of STA among the observers was relatively large. This finding highlights the subjectivity that takes place when tracing/marking anatomical structures on cephalograms, even when observers are trained and calibrated. Because of the large range among the observers, the results were presented observer-wise, and not as a consensus. However, independent of the observer, the range of STA in images acquired with simulated movements was larger than in images acquired without movement. This was more obvious for images acquired in D-3 and ORT.

To optimize the study design, the differences in STA and S were calculated case-wise, and for every two images acquired with movement, there was a no-movement control image. The differences in focal distance, image resolution, and field of view among the tested cephalostats did not allow a direct comparison of the values obtained in pixels and pixels^2. In other words, the obtained values could not be converted into millimeters. Thus, to provide a better understanding of the results, Diff-STA and Diff-S were also calculated as a percentage in relation to the corresponding average values for the control images. The fact that the amount of negative and positive Diff-STA values was almost equal indicates a wide range in STA values due to movements and differences in the cephalostats. For Diff-S, the average sella turcica diameter in control images was served as a reference for comparison. Axelsson et al. describe that this parameter is commonly used in the determination of STA and shape.[7] Based on the literature, differences in *S* location, which are larger than 10% of the sella turcica diameter, could already lead to substantial differences in the cephalometric angular measurement values.[4,14,18,19] Therefore, the value of 10% was taken as the threshold for relevant variations in sella location. Overall, Diff-S varied as seen for Diff-STA, except for ORT, where a large number of cases were associated with extreme values. Not only the changes in STA, but also the misshaping of sella turcica led to a large variation in the identification of *S*. These changes, which were related to the presence of movement, are in agreement with what was previously suggested in the literature by Svystun et al.[11]

This was a pilot study based on a single skull. Evidently, the present results include method- and observer-related errors that are part of all types of cephalometric analyses. Also, the influence of skull morphology on the results was not considered. This must be listed as a limitation. On the contrary, one could also list this as an advantage since the influence of biological diversity was eliminated as a factor, leading to a broader range in the measurements. Future studies based on a larger sample of skulls should take biological diversity into consideration, defining the factors that influence the measurement outcome the most. Also, real soft tissue was absent in the skull, eliminating the errors that could be associated with the soft tissue summation in the cephalogram.[25]

Knowing that patient movement may be a considerable factor causing serious changes in landmark location, one could speculate that it influences the diagnosis and treatment planning in orthodontics. This would be the ultimate clinical relevance of the present results. Our study, however, does not serve to speculate if cephalograms acquired in the presence of movement may present challenges when other peripheral cephalometric points are to be localized. Sella turcica is a central anatomical structure in the skull, and therefore the impact of distortion-related artifacts might be different than for more peripheral points. Also, differences in the location of multiple landmarks are combined during cephalometric analysis, which might increase the magnitude of discrepancy. Further studies highlighting the impact of patient movement and patient motion artifacts on the results of a complete cephalometric analysis are needed to define the clinical impact of the current findings. The present results should also be taken into consideration when developing artificial intelligence tools or deep-learning algorithms to automatize cephalometric tracing. The reported distortions could be a factor that may affect the outcome of automatized solutions for cephalometric analysis.

Conclusion

Simulated head movements caused significant distortion in lateral cephalograms acquired by CCD-based cephalostats, as seen from alterations in STA and location of the cephalometric point sella. The results were dependent on the presence of movement and, for D-3 and D-4, movement type and pattern.

References

1. Tekiner H, Acer N, Kelestimur F. Sella turcica: an anatomical, endocrinological, and historical perspective. Pituitary 2015;18(4):575–578. DOI: 10.1007/s11102-014-0609-2.
2. Jones RM, Faqir A, Millett DT, et al. Bridging and dimensions of sella turcica in subjects treated by surgical-orthodontic means or orthodontics only. Angle Orthod 2005;75(5):714–718. DOI: 10.1043/0003-3219(2005)75.
3. Muhammed FK, Abdullah AO, Liu Y. Morphology, incidence of bridging, dimensions of sella turcica, and cephalometric standards in three different racial groups. J Craniofac Surg 2019;30(7):2076–2081. DOI: 10.1097/SCS.0000000000005964.
4. Axelsson S, Storhaug K, Kjaer I. Post-natal size and morphology of the sella turcica. Longitudinal cephalometric standards for Norwegians

between 6 and 21 years of age. Eur J Orthod 2004;26(6):597–604. DOI: 10.1093/ejo/26.6.597.
5. Zagga AD, Ahmed H. Plain radiographic cephalometry of the sella turcica: an overview. Niger J Med 2008;17(3):333–336.
6. Bjork A, Solow B. Measurement on radiographs. J Dent Res 1962;41:672–683. DOI: 10.1177/00220345620410032101.
7. Axelsson S, Kjaer I, Bjornland T, et al. Longitudinal cephalometric standards for the neurocranium in Norwegians from 6 to 21 years of age. Eur J Orthod 2003;25(2):185–198. DOI: 10.1093/ejo/25.2.185.
8. Gandikota CS, Rayapudi N, Challa PL, et al. A comparative study of linear measurements on facial skeleton with frontal and lateral cephalogram. Contemp Clin Dent 2012;3(2):176–179. DOI: 10.4103/0976-237X.96823.
9. Chadwick JW, Prentice RN, Major PW, et al. Image distortion and magnification of 3 digital CCD cephalometric systems. Oral Surg Oral Med Oral Pathol Oral Radiol Endod 2009;107(1):105–112. DOI: 10.1016/j.tripleo.2008.09.025.
10. Svystun O, Schropp L, Wenzel A, et al. Prevalence and severity of image-stitching artifacts in charge-coupled device-based cephalograms of orthodontic patients. Oral Surg Oral Med Oral Pathol Oral Radiol 2020;129(2):158–164. DOI: 10.1016/j.oooo.2019.07.004.
11. Svystun O, Wenzel A, Schropp L, et al. Image-stitching artefacts and distortion in CCD-based cephalograms and their association with sensor type and head movement: ex vivo study. Dentomaxillofac Radiol 2020;49(3):20190315. DOI: 10.1259/dmfr.20190315.
12. Spin-Neto R, Wenzel A. Patient movement and motion artefacts in cone beam computed tomography of the dentomaxillofacial region: a systematic literature review. Oral Surg Oral Med Oral Pathol Oral Radiol 2016;121(4):425–433. DOI: 10.1016/j.oooo.2015.11.019.
13. Schropp L, Alyass NS, Wenzel A, et al. Validity of wax and acrylic as soft-tissue simulation materials used in in vitro radiographic studies. Dentomaxillofac Radiol 2012;41(8):686–690. DOI: 10.1259/dmfr/33467269.
14. McIntyre GT, Mossey PA. Size and shape measurement in contemporary cephalometrics. Eur J Orthod 2003;25(3):231–242. DOI: 10.1093/ejo/25.3.231.
15. Kunz F, Stellzig-Eisenhauer A, Zeman F, et al. Artificial intelligence in orthodontics: evaluation of a fully automated cephalometric analysis using a customized convolutional neural network. J Orofac Orthop 2020;81(1):52–68. DOI: 10.1007/s00056-019-00203-8.
16. Chen Yj CS, Huang HW, Yao CC, et al. Reliability of landmark identificationin cephalometric radiography aquired by a storage phosphor imaging system. Dentomaxillofac Radiol 2004;33(5):1259. DOI: 10.1259/dmfr/85147715.
17. Riedel RA. The relation of maxillary structures to cranium in malocclusion and in normal occlusion. Angle Orthodontist 1952;22(3):142–145.
18. Devereux L, Moles D, Cunningham SJ, et al. How important are lateral cephalometric radiographs in orthodontic treatment planning? Am J Orthod Dentofacial Orthop 2011;139(2):e175–e181. DOI: 10.1016/j.ajodo.2010.09.021.
19. Steiner CC. Cephalometrics for you and me. Am J Orthod Dentofac 1953;39(10):729–755. DOI: 10.1016/0002-9416(53)90082-7.
20. Schulze R, Heil U, Gross D, et al. Artefacts in CBCT: a review. Dentomaxillofac Radiol 2011;40(5):265–273. DOI: 10.1259/dmfr/30642039.
21. Durão AP, Morosolli A, Pittayapat P, et al. Cephalometric landmark variability among orthodontists and dentomaxillofacial radiologists: a comparative study. Imaging Sci Dent 2015;45(4):213–220. DOI: 10.5624/isd.2015.45.4.213.
22. Oktay H. A comparison of ANB, WITS, AF-BF, and APDI measurements. Am J Orthod Dentofacial Orthop 1991;99(2):122–128. DOI: 10.1016/0889-5406(91)70114-C.
23. Huh KH, Benavides E, Jo YT, et al. Quantitative evaluation of patient movement during simulated acquisition of cephalometric radiographs. J Digit Imaging 2011;24(3):552–559. DOI: 10.1007/s10278-010-9318-1.
24. Spin-Neto R, Matzen LH, Hermann L, et al. Head motion and perception of discomfort by young children during simulated CBCT examinations. Dentomaxillofac Radiol 2020:20200445. DOI: 10.1259/dmfr.20200445.
25. Hagg U, Cooke MS, Chan TC, et al. The reproducibility of cephalometric landmarks: an experimental study on skulls. Aust Orthod J 1998;15(3):177–185.